THE JOURNAL OF PHYSICAL CHEMISTRY A

Article

pubs.acs.org/JPCA

Experimental Evidence of Long-Range Intramolecular Vibrational Energy Redistribution through Eight Covalent Bonds: NIR Irradiation Induced Conformational Transformation of *E*-Glutaconic Acid

Benjámin Kovács,[†] Nihal Kuş,[‡,§] György Tarczay,*[,†] and Rui Fausto*[,‡]

[†]Institute of Chemistry, Eötvös University, PO Box 32, H-1518 Budapest 112, Hungary

[‡]CQC, Department of Chemistry, University of Coimbra, 3004-535 Coimbra, Portugal

[§]Department of Physics, Anadolu University, TR-26470 Eskişehir, Turkey

Supporting Information

ABSTRACT: Long-range intramolecular vibrational energy redistribution (IVR) driven conformational changes were investigated in a matrix-isolated open-chain, asymmetrical dicarboxylic acid, *E*-glutaconic acid. Although the analysis was challenging due to the presence of multiple backbone conformers and short lifetimes of the prepared higher energy *cis* conformers, it was shown that the selective excitation of the O−H stretching overtone of one of the carboxylic groups can induce the conformational change (*trans* to *cis*) of the other carboxylic group, located at the other end of the *E*-glutaconic acid molecule. This is a direct proof that the IVR process can act through eight covalent bonds in a flexible molecule before the excess energy completely dissipates into the matrix. The lifetime of the prepared higher energy conformers (averaged over the different backbones) was measured to be 12 s.

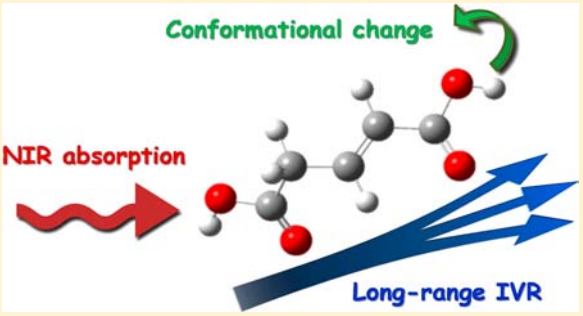

1. INTRODUCTION

The detailed understanding of photochemical processes at the molecular level requires not only the investigation of the excitations but also the relaxation mechanisms. The excess energy of vibrationally excited molecules can be dissipated via either inter- or intramolecular relaxation pathways. The theoretical interpretation of the intermolecular relaxation processes is grounded on a solid base,[1] while the background of intramolecular vibrational energy redistribution (IVR) is far more complicated.[2] Therefore, the experimental investigations of the IVR phenomenon have a great importance.

Although there are experimental examples of direct observation of IVR processes in condensed phase, e.g., in solution,[3] IVR can be best studied in the gas phase[4−6] or in the case of nearly isolated molecules, because under these conditions the intermolecular relaxation processes are negligible. Even in this case, a proper environment can enhance the effect, serving as a buffer for compensating the energy gap between the vibrational levels. From this perspective, the matrix isolation method offers ideal conditions for studying IVR processes.[7−9] This method also provides well-resolved vibrational spectra, making conformational assignments possible.

It was demonstrated by many studies that excitation of the overtones and combination vibrational modes by narrow band NIR or MIR laser irradiations can induce conformational transformations of a selected conformer in a matrix-isolated molecule.[10−12] These transformations are driven by the IVR processes between the excited vibrational levels and a highly excited torsional mode along the reaction coordinate. A very effective NIR induced conformation transformation, the *cis*−*trans* (or *Z*−*E*) conversion of the carboxylic group, occurs when the first overtone of the OH stretching is pumped by a laser.[10−15] Indeed, though in this case the vibrational excitation is not strictly local, because the excited vibrational coordinate is not the same as the one defining the conformational changes (for example, for formic and acetic acids, pumping of the OH stretching overtone led to geometry changes occurring along the CCOH torsion coordinate), the coordinates responsible for the conformational changes are located closely in space in relation to the excited fragment.

As an early demonstration of nonlocal or remote pumping, it was shown that the excitation of CH (CH_3) and CO stretching overtones can also induce *cis*−*trans* conformational change in formic and acetic acid.[13−15] More recent examples include amino acids. The irradiation of the first overtone of the NH stretching mode of glycine results in the *cis*−*trans* conversion of the carboxylic group,[16] while the excitation of the first overtone of the OH stretching mode of the carboxylic OH group can induce a conformational change in the side chain in serine.[17] Although in these two latter examples the energy is absorbed by a group different from the group in which the conformational change occurs, these groups are spatially close to each other;

Received: January 19, 2017
Revised: April 17, 2017
Published: April 19, 2017

DOI: 10.1021/acs.jpca.7b00615
J. Phys. Chem. A XXXX, XXX, XXX−XXX

therefore, the conformational change might occur due to noncovalent interactions (e.g., due to H-bond or spatial hindrance) and not by a so-called long-range IVR process. More obvious examples of long-range IVR processes were observed recently for 2-thiocytosine, in which SH rotamerization was induced by the excitation of the NH_2 stretching overtone;[7] in kojic acid, in which the phenolic OH group was irradiated and the conformational change of the hydroxymethyl group was observed;[8] and in 6-methoxyindole, in which the excitation of the NH stretching overtone induced the conformational change of the methoxy group.[9] In each of these examples, the two groups are connected by aromatic rings, which can facilitate the IVR process. Finally, it is interesting to note that an intermolecular vibrational energy redistribution process was observed through a hydrogen bond in matrix-isolated formic acid dimers.[18]

The aim of the present study is to reveal the long-range IVR in a more flexible, nonaromatic molecule. The molecule selected for this purpose, *E*-glutaconic acid, unequivocally has a structure different from those examined previously. *E*-glutaconic acid has two carboxylic groups, and due to the asymmetric position of a C═C double bond, these two groups are distinguishable. In this paper, to differentiate between the two carboxyl groups (and the respective OH or CO groups) of the molecule, the carboxylic group located closer to the C═C double bond is denoted by **1**, and the other one by **2**. Regarding the *cis*−*trans* conformations of the carboxylic groups, the first denomination refers to **1**, and the second one refers to the conformation of the carboxylic group **2**. (Note that the literature is not consistent in the *cis*−*trans* nomenclature of a carboxylic group. The nomenclature used in the present study is given in Figure 1.) The asymmetry of this molecule enables

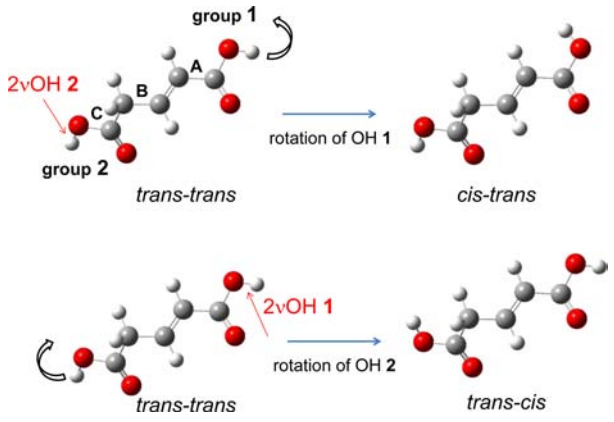

Figure 1. Nomenclature in *E*-glutaconic acid used in this paper and the long-range IVR driven processes intended to be observed.

one to selectively excite vibrationally one of its carboxylic groups and detect the conformational change of the other group by IR spectroscopy. The processes intended to be observed are summarized in Figure 1.

2. COMPUTATIONAL DETAILS

The elucidation of the experimental results was supported by quantum mechanical computations. Geometry optimizations were performed at the B3LYP[19,20]/6-31++G**[21−23] and MP2[24]/6-311++G** levels of theory. Transition structures between different conformers were located by the synchronous transit-guided quasi-Newton (STQN)[25] method. Fundamental vibrational wavenumbers and IR transition intensities were computed by two different methods. In the first method, the B3LYP/6-31++G** harmonic frequencies were empirically improved by the scaled quantum mechanical (SQM)[26,27] approach, using the scaling factors determined by Fábri et al. for spectra recorded in an Ar matrix.[28] In the second method, vibrational anharmonicities were taken into account by second-order vibrational perturbation theory. The latter method was used to compute the wavenumbers of the overtone transitions too. The computations were carried out using the Gaussian 09[29] and PQS[30,31] program packages.

3. EXPERIMENTAL DETAILS

E-Glutaconic acid was obtained from Sigma-Aldrich, purity >97%. For matrix deposition, the solid sample was placed in a specially designed Knudsen cell heated up to 350 K. The vapor was codeposited on a CsI window with a large excess of Ar or N_2 gas (purity N60 and N48, respectively). The CsI substrate was kept at 11−14 K either by an APD Cryogenics DE-202A closed-cycle helium refrigerator system or Janis CCS-350R cold head cooled by a CTI Cryogenics 22 refrigerator.

The mid-infrared (MIR) spectra were recorded, with 1 cm^{-1} spectral resolution, using a Bruker IFS 55 FT-IR spectrometer equipped with a liquid-N_2-cooled mercury and cadmium telluride (MCT) detector, a KBr beam splitter, and a Globar source. In the near-infrared (NIR), spectra were recorded on a Thermo Nicolet 6700 spectrometer. In the NIR spectral range, a CaF_2 beam splitter, a tungsten lamp source, and an InGaAs detector were used.

Conformational changes were selectively induced by an optical parametric oscillator (VersaScan MB 240 OPO, GWU/Spectra Physics) pumped with the third harmonic (355 nm) of a pulsed (10 Hz, 2−3 ns) Quanta Ray Lab 150 Nd:YAG laser (Spectra Physics). The line width of the idler (NIR) output of the OPO was about 5 cm^{-1}, and pulse energies were 4−10 mJ. The laser beam was unfocused; its diameter was about 0.8 cm. In order to record the spectra during the laser irradiation, an LPW 3860 low pass filter was placed between the cold window and the detector.

For recording the spectra of conformers with short lifetimes, first a 64 scan (90 s) averaged spectrum was taken. Then, the laser was turned on, and after waiting 30 s to reach the steady state concentration of the short-lived conformer, a second 64 scan averaged spectrum was recorded during the laser irradiation. Finally, the laser was switched off, and after waiting 30 s, a third 64 scan averaged spectrum was collected. (Technically, it is not advantageous to accumulate longer, because in the difference spectra the stable site-changing species will dominate over the short-lived *trans*−*cis* forms.) In order to visualize the spectra corresponding to the short-lived conformer, difference spectra were computed from the spectra recorded during and before the irradiation, as well as from the spectra taken after and before the irradiation. The positive bands observed only in the first difference spectrum correspond to the short-lived conformers. In order to improve the signal-to-noise ratio, this process was repeated 20 times, and the difference spectra were averaged; this means a 30 min cumulative accumulation time.

For lifetime measurements, single interferograms were scanned with a repetition rate of 4.3 s. The laser radiation was switched on at the beginning of a 45 scan cycle, and it was switched off after the 24th scan; i.e., the 25−45th scans were recorded in the dark. This cycle was repeated 50 times, and the

DOI: 10.1021/acs.jpca.7b00615
J. Phys. Chem. A XXXX, XXX, XXX−XXX

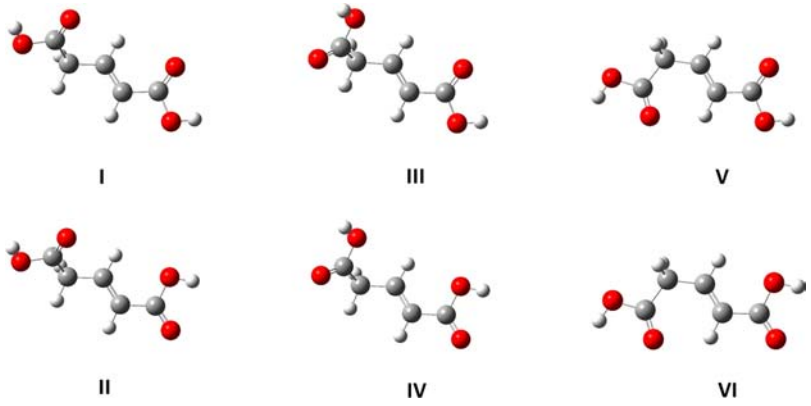

Figure 2. Six (*trans*−*trans*) conformers that, according to the B3LYP/6-31++G** level of theory, have at least 1% abundance in the vapor phase at 350 K.

corresponding interferograms from each cycle were averaged and Fourier-transformed.

4. RESULTS AND DISCUSSION

4.1. Identification of the Isomers of the Deposited Sample. In order to assign the NIR spectra, to select the appropriate wavelengths for the irradiations to perform, and to understand the NIR laser-induced conformational changes, the conformational landscape of *E*-glutaconic acid has to be explored first. This is followed by the computation of the vibrational spectra of the conformers in both the MIR and NIR regions. It shall be stressed here that not only the internal rotations within the two carboxylic acid groups (along the C—O bond) but also the rotations along the three single C—C bonds contribute to the conformational flexibility of the molecule. The latter are here denoted by **A**, **B**, and **C**: **A** is connected to carboxylic group **1**, **C** to **2**, and **B** is the middle C—C bond. The rotation along the C═C double bond has a high barrier, and therefore, this rotation was not considered in the conformational search.

Initial geometries for the conformational search were prepared by varying the torsional angles corresponding to **A**, **B**, and **C** by 120°. This, combined with the possible *cis* and *trans* orientations of the two carboxylic groups, resulted in 2·2·3·3·3 = 108 initial structures. After geometry optimization, the Gibbs free energies relative to the most stable conformer and the mole fractions were determined for the sample evaporation temperature, 350 K. As depicted in Figure 2, B3LYP/6-31++G** computations predict six conformers with at least 1% abundance at 350 K. Both carboxylic groups of each of these conformers have a *trans* structure. The backbone conformations are denoted by roman numbers, in decreasing mole fraction order. Table 1 summarizes the computed Gibbs free energies and mole fractions for these conformers, as well as for the most stable *cis*−*trans*, *trans*−*cis*, and *cis*−*cis* forms.

In general, higher energy conformers that are separated from a more stable conformer by low-energy (≈5 kJ mol^{-1} or lower) barriers can partially or completely convert to the lower energy forms upon matrix deposition.[32] Therefore, the possible transition structures between the six most stable conformers, i.e., the six *trans*−*trans* conformers of *E*-glutaconic acid, were located on its potential energy surface. These barrier heights are summarized in Table 2. As can be seen, all of these barriers are high enough to prevent conformational conversions from taking place during the deposition of the matrix.

Table 1. Relative Gibbs Free Energies ($\Delta G^{\circ}_{r,350K}$) and Mole Fractions of the Six *trans*−*trans* Conformers at 350 K and Those of the Corresponding *cis*−*trans*, *trans*−*cis*, and *cis*−*cis* Forms

conformer	$\Delta G^{\circ}_{r,350K}$ (kJ·mol^{-1})	mole fraction
I (*trans*−*trans*)	0.0	0.35
II (*trans*−*trans*)	1.0	0.25
III (*trans*−*trans*)	1.6	0.20
IV (*trans*−*trans*)	3.2	0.12
V (*trans*−*trans*)	3.9	0.05
VI (*trans*−*trans*)	5.7	0.03
most stable *trans*−*cis*	23.7	5.2×10^{-5}
most stable *cis*−*trans*	26.7	1.7×10^{-5}
most stable *cis*−*cis*	49.5	7.2×10^{-9}

Table 2. Zero-Point Vibrational Energy Corrected Barrier Heights between the *trans*−*trans* Conformers as Obtained at the B3LYP/6-31++G Level of Theory**

conversion	rotation	barrier height (kJ·mol^{-1})
trans **IV** → *trans* **II**	C	10.5
trans **III** → *trans* **I**	C	9.1
trans **II** → *trans* **I**	A	29.8
trans **IV** → *trans* **III**	A	29.2
trans **VI** → *trans* **V**	A	28.5

A comparison between the computed and experimentally observed OH and CO stretching fundamental regions is shown in Figure 3, and the corresponding vibrational wavenumbers are collected in Tables 3 and 4. Complete unambiguous assignment cannot be made, because of the close vicinity of the bands, possible site splits, and spectral overlaps. However, the experimental spectra clearly show that several conformers are present. Furthermore, both the SQM and the VPT computations indicate that, for each of the six *trans*−*trans* conformers, the OH stretching fundamental of carboxylic group **1** appears at a higher frequency than that of carboxylic group **2**, while the opposite is true for the CO stretching fundamental; i.e., it appears at a higher wavenumber in the case of carboxylic group **2**. Although we cannot completely exclude that there is no large site splitting (>10−15 cm^{-1}) in the OH region, three observations suggest that in the present case we do not need to count with the possible interferences of site splitting for the data analysis. First, the computed spectra (that do not take into account the sites) fit very well to the experimental spectra in

DOI: 10.1021/acs.jpca.7b00615
J. Phys. Chem. A XXXX, XXX, XXX−XXX

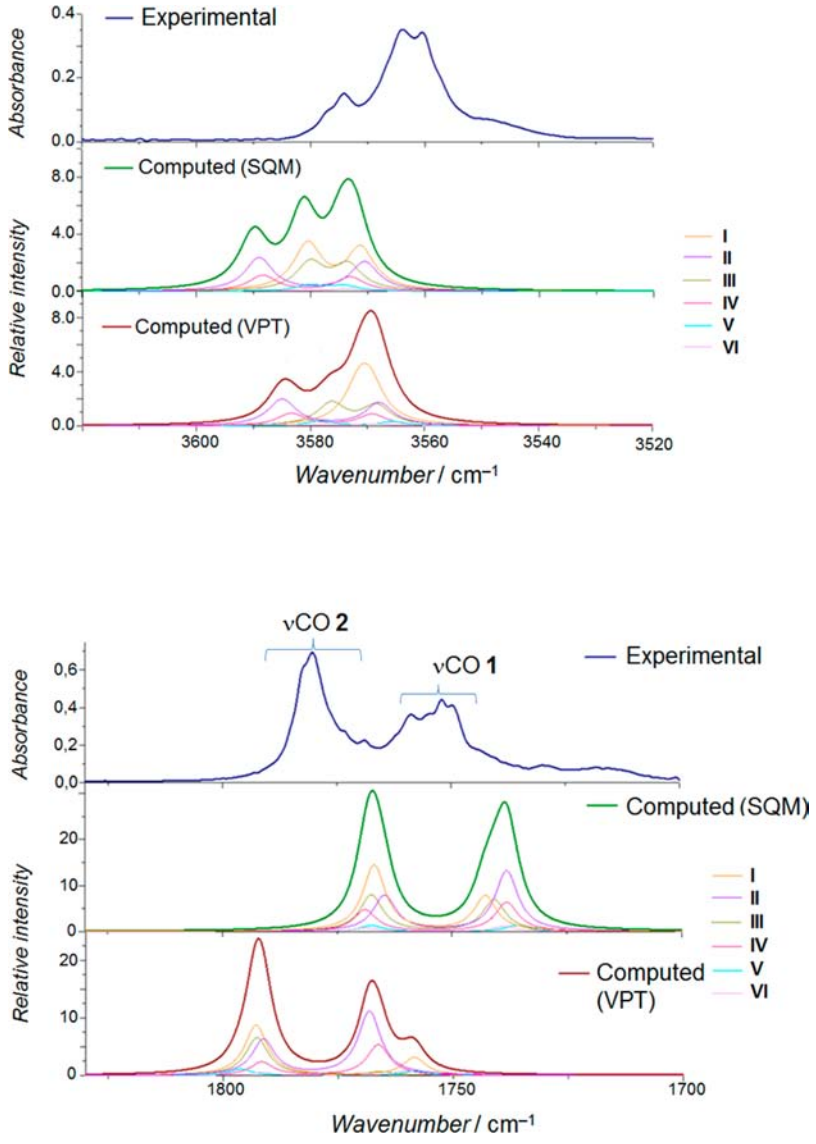

Figure 3. OH and CO stretching regions of the computed and experimental spectra recorded in an Ar matrix.

Table 3. Computed Wavenumbers (in cm^{-1}) of the OH Stretching Fundamental Modes of the Six *trans–trans* Conformers with Tentative Assignments to Experimental MIR Bands

backbone conformation	νOH 1			νOH 2		
	SQM[a]	VPT2[a]	Exp.[b]	SQM[a]	VPT2[a]	Exp.[b]
I	3580	3571	3564	3571	3569	3564
II	3589	3585	3577[c]	3570	3568	3560
III	3580	3576	3567[c]	3573	3568	3560
IV	3588	3583	3574	3573	3569	3560
V	3580	3578	3567[c]	3574	3565	3558[c]
VI	3590	3586	3577[c]	3574	3569	3560

[a]B3LYP/6-31++G**. [b]Ar matrix. [c]Shoulder.

Table 4. Computed Wavenumbers (in cm^{-1}) of the CO Stretching Fundamental Modes of the Six *trans–trans* Conformers with Tentative Assignments to Experimental MIR Bands

backbone conformation	νCO 1			νCO 2		
	SQM[a]	VPT2[a]	Exp.[b]	SQM[a]	VPT2[a]	Exp.[b]
I	1743	1758	1749, 1752	1767	1793	1780
II	1738	1768	1755, 1759	1765	1791	1780
III	1741	1766	1755, 1759	1768	1793	1780
IV	1738	1766	1755, 1759	1769	1792	1780
V	1736	1758	1749, 1752	1767	1796	1782
VI	1738	1760	1749, 1752	1769	1792	1780

[a]B3LYP/6-31++G**. [b]Ar matrix. The assignments to different backbones are uncertain due to site splittings.

the OH stretching and in the first OH stretching overtone region. Second, the experimental spectra in the OH stretching and in the first OH stretching overtone regions (see below) are very similar, while in the case of site splitting we would expect different anharmonicities for different sites. Third, the herein proposed band assignments for the two regions allow a clear, consistent interpretation of the results. Of course, smaller site splittings (a few cm^{-1}) are very likely present, which, besides the existence of multiple backbone conformers, are responsible for the broadening of the OH stretching bands.

DOI: 10.1021/acs.jpca.7b00615
J. Phys. Chem. A XXXX, XXX, XXX−XXX

The spectral patterns of other regions of the MIR spectrum are also well reproduced by the calculations (see the Supporting Information), but similarly to the OH and CO stretching regions, the corresponding vibrations of the six lower energy conformers of *E*-glutaconic acid have wavenumbers that are very close to each other; therefore, no complete and unambiguous conformational assignment can be made.

As can be seen in Figure 4, there are four dominant bands in the spectral region corresponding to the first overtone of the

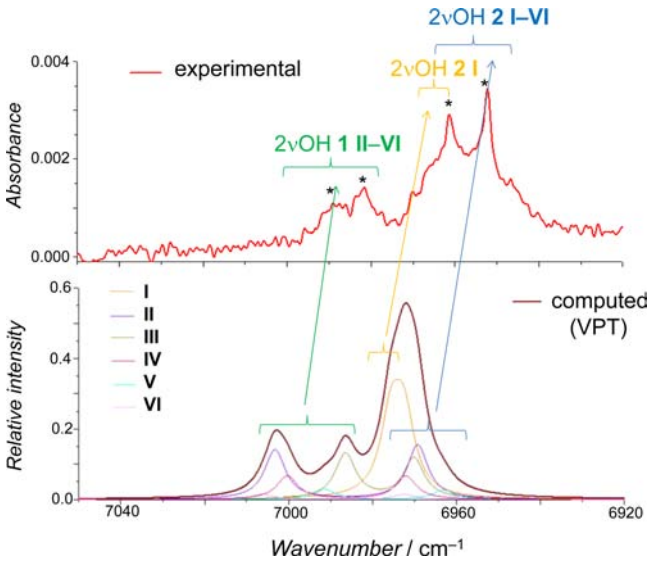

Figure 4. Assignments of the OH stretching overtone region. The experimental spectrum is recorded in an Ar matrix. The positions of the NIR laser irradiations are marked with asterisks.

OH stretching mode (2νOH). Each of these bands has shoulders, revealing the complexity due to the presence of six conformers and two carboxylic OH groups for each conformer. According to the VPT2 computations (see Table 5), the two

Table 5. Computed Wavenumbers (in cm^{-1}) of the First Overtone of the OH Stretching Mode of the *trans*−*trans* Conformers with Tentative Assignments to Experimental NIR Bands

	2νOH **1**		2νOH **2**	
backbone conformation	VPT2[a]	Exp.[b]	VPT2[a]	Exp.[b]
I	6975	6965[c]	6972	6961
II	7003	6989	6969	6952
III	6986	6982	6970	6952
IV	7000	6989	6972	6961
V	6991	6982	6963	6952
VI	7006	6989	6972	6961

[a]B3LYP/6-31++G**. [b]Ar matrix. [c]Shoulder.

lower intensity bands at higher wavenumbers (6982 and 6989 cm^{-1}) unambiguously correspond to the 2νOH mode of the carboxylic group of **1** of the *trans*−*trans* conformers with backbone **II** to **VI**. The intensive and relatively sharp band at 6952 cm^{-1} can also be assigned confidently; it belongs to the 2νOH mode of carboxylic group **2** of the *trans*−*trans* conformers with backbone **II**, **III**, **IV**, and **VI**, and possibly also **V**. Finally, the similarly intense but broader band at 6961 cm^{-1} corresponds most likely to both 2νOH bands (i.e., **1** and **2**) of the *trans*−*trans* conformer **I**, because for this conformer the computed wavenumber difference between the 2νOH **1** and 2νOH **2** bands is only 3 cm^{-1}. The 2νOH **2** mode of *trans*−*trans* **II**, **III**, **IV**, **V**, and **VI** conformers might also contribute to this band. Considering the above assignments and our laser line width, it can be concluded without determining the accurate conformational distribution that upon 6982 and 6989 cm^{-1} irradiation only carboxylic group **1** is excited, while upon irradiation at 6952 cm^{-1} only carboxylic group **2** can absorb a photon. On the other hand, the 6961 cm^{-1} photons might be absorbed by both groups. In practice, the laser wavelength was optimized for the most efficient bleaching. This optimization resulted in irradiation wavenumbers of 6991, 6985, 6965, and 6955 cm^{-1}, according to the reading of the OPO controller. Since these wavenumbers are systematically 2−3 cm^{-1} higher than the band maxima in the NIR spectrum, the differences are mostly due to the imprecise calibration of the OPO. Therefore, hereafter we will refer to the measured band positions of the NIR spectra, and not to the OPO reading, as the irradiation wavenumbers.

The effects of the irradiations were examined by the analysis of the MIR spectra. The difference spectra obtained by subtracting the spectra recorded before the irradiations from the ones recorded during the irradiations (red traces) and the difference spectra obtained by subtracting the spectra recorded before the irradiations from the one recorded 90 s after the end of the irradiations (blue traces) are shown in Figure 5. The positive bands in the latter type of difference spectra (blue traces) correspond to species with longer (>60 s) lifetime, while in the other type (red traces) mostly the bands of short-lived species are expected, with some possible contribution from the (more) stable species.

As can be seen from the blue traces of Figure 5, spectral changes that are not restored in 90 s after switching off the laser can only be observed in the carbonyl stretching region (exceptions are for two very weak bands at 1189 and 1361 cm^{-1} appearing upon the 6982 and 6989 cm^{-1} irradiations). The very high relative intensity of the CO stretching bands results in relatively intense bands in the difference spectra. The complicated pattern in the carbonyl stretching region, between ca. 1750 and 1775 cm^{-1}, is most likely due to very small changes in the matrix sites.

Similar difference patterns were observed upon irradiations of several minutes and hours. This means that these irradiations do not promote the formation of stable conformers from other stable forms. These observations also indicate that (1) the conformational transformation of the backbone is unfeasible in the low-temperature, rigid matrix due to steric effects; (2) if *cis*−*trans*, *trans*−*cis*, or *cis*−*cis* conformers are formed, then their lifetime is less than ca. 1 min. Note that, according to literature data, the lifetime of a *cis* carboxylic acid form can be as short as 7 s in a 10−12 K Ar matrix, due to fast H-tunneling.[33]

The red traces in Figure 5 indicate that even though stable species are not generated short-lived species are being formed, because many bands are observed only during the irradiations. The most intense bands of the short-lived species appeared in the 1232−1272, 1274−1309, and 1793−1814 cm^{-1} regions for each irradiation, and, in addition, at 1326 cm^{-1} in the case of the 6961 cm^{-1} irradiation. Among these, the most intense bands are those observed between 1793 and 1814 cm^{-1}, which belong to the CO stretching mode of the short-lived species.

In order to assign these bands to short-lived conformers, the following assumptions were made. First, considering that

DOI: 10.1021/acs.jpca.7b00615
J. Phys. Chem. A XXXX, XXX, XXX−XXX

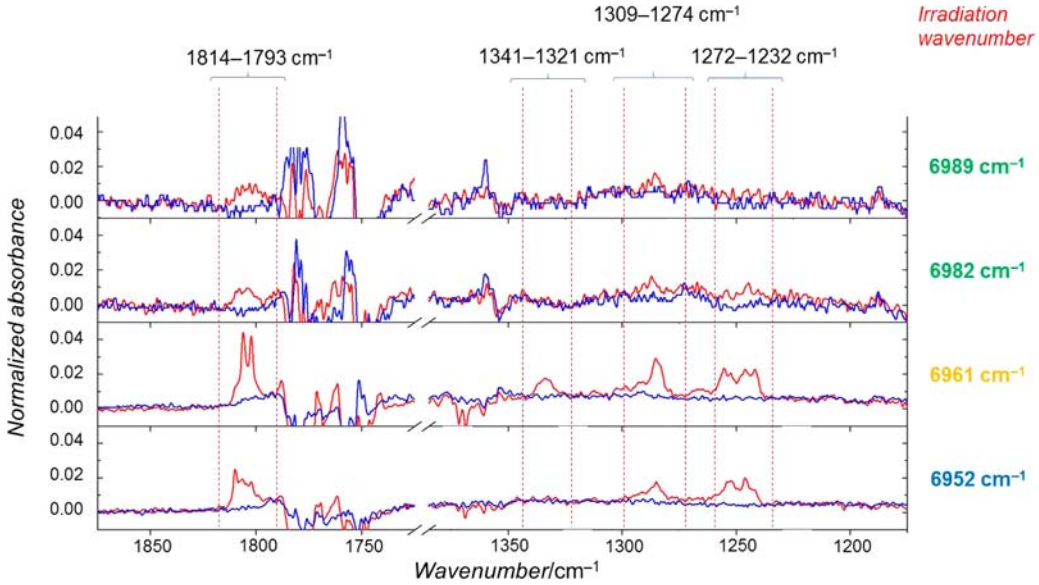

Figure 5. Difference spectra of the spectra of the transient species, i.e., the spectra obtained by subtracting the spectra recorded before the irradiation from the ones recorded during the irradiations (red traces), and the difference spectra obtained by subtracting the spectra recorded before the irradiation from the one recorded after the irradiations (blue traces). The wavenumbers of the irradiations are given on the right. Spectra were recorded in an Ar matrix. The intensities are normalized by the absorption intensity of the irradiated 2νOH bands; from top to bottom: 0.00319, 0.00585, 0.02195, 0.0225.

during the irradiation only ~0.1% of the *trans*–*trans* form is converted to short-lived (*X-cis* and *cis-X*, *X* = *trans* or *cis*) forms and assuming a similar efficiency for the absorption of a second photon and for the *trans* to *cis* conversion of the *X-cis* and *cis-X*, we expect <0.0001% two-step conversion to the *cis*–*cis* form, which is below our detection level. It is also unlikely that the absorption of a single photon can cause conformational change on both carboxylic groups with a quantum yield that could produce enough *cis*–*cis* conformers for detection. Therefore, the analysis can be restricted to the *cis*–*trans* and *trans*–*cis* conformers, while the *cis*–*cis* conformers can be excluded. Second, as was already mentioned, the irradiations cannot effectively induce conformational changes of the backbone. Hence, only the *cis*–*trans* and *trans*–*cis* conformers with backbones **I**–**VI** are considered in the following discussion. In order to compute their vibrational frequencies, these 2 × 6 structures were generated from the corresponding *trans*–*trans* forms by changing the CCOH torsion angle from 180 to 0° and then reoptimized at the B3LYP/6-31++G** level of theory. The SQM B3LYP/6-31++G** wavenumbers of the CO stretching fundamentals of the obtained conformers are collected in Table 6.

Table 6. Computed (SQM B3LYP/6-31++G) CO Stretching Fundamental Wavenumbers (in cm^{-1}) of *cis*–*trans* and *trans*–*cis* Conformers with Backbone I–VI**

	cis–*trans*		*trans*–*cis*	
backbone conformation	νCO **1**	νCO **2**	νCO **1**	νCO **2**
I	1775	1766	1745	1799
II	1765	1759	1739	1797
III	1771	1767	1744	1794
IV	1763	1773	1742	1795
V	1768	1762	1736	1799
VI	1769	1767	1741	1800

As the data shown in Table 6 and Figure 6 show, the CO stretching fundamentals of the *trans*–*cis* and *cis*–*trans* conformers are clustered into three groups. Independently from the backbone conformation, the computed νCO **2** wavenumber of the *trans*–*cis* conformers is 50–60 cm^{-1} higher than that corresponding to νCO **1**. In contrast to this, the two fundamental νCO modes of the *cis*–*trans* conformers are very close to each other, and they depend considerably on the backbone conformation. According to the computations, both fundamental νCO modes of all *cis*–*trans* conformers have wavenumbers staying between and very well separated from those of the two fundamental νCO modes of the *trans*–*cis* conformers. Furthermore, the higher wavenumber νCO fundamental mode of the *cis*–*trans* conformers overlaps with the νCO fundamental of the *trans*–*trans* conformers (see Table 4), while the lower wavenumber νCO fundamental mode overlaps with the lower wavenumber νCO fundamental mode of the *trans*–*cis* conformers. As a conclusion, independently from the backbone conformation, the νCO **2** bands of the *trans*–*cis* conformers at very high wavenumbers are distinctive, and can be used for the identification of conformers with *trans*–*cis* carboxylic groups.

As was mentioned before, and can be seen in Figure 5, bands of short-lived conformers were observed between 1793 and 1814 cm^{-1} in each irradiation. These bands can unambiguously be assigned to the νCO **2** mode of the *trans*–*cis* conformers. This means that, although in the case of the 6982 and 6989 cm^{-1} irradiation experiments only carboxylic group **1** can absorb the photons, the conformation change takes place on carboxylic group **2**. This proves that the IVR process can act through eight covalent bonds in a flexible molecule, before the excess energy completely dissipates into the matrix. In order to eliminate the effect of different absorptions at different irradiation wavelengths, in Figure 5, the spectra were normalized by the absorption intensities of the irradiated bands. As seen, the "remote pumping" is only a few times less effective than the "local pumping". This difference is not

DOI: 10.1021/acs.jpca.7b00615
J. Phys. Chem. A XXXX, XXX, XXX–XXX

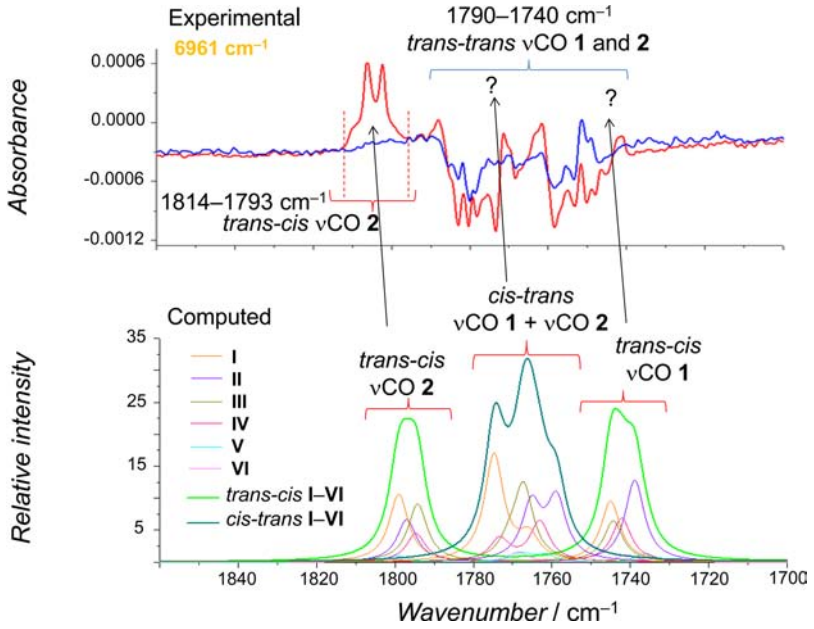

Figure 6. Assignment of the CO stretching region of spectra (recorded in an Ar matrix) of the transient species.

surprising, and can be rationalized by the competitive energy transfer to the matrix. Furthermore, the efficiency of "remote pumping" compared to that of "local pumping" is much larger than could be caused by nonresonant effects (i.e., pumping of a combination of molecular vibrational and lattice modes; see below) or by the line width of our laser radiation. It should also be noted that the band structures in the 1793−1814 cm^{-1} region look different for the different irradiations, which results from the fact that the overlap of the 2νOH band of the different backbone conformers with the excitation laser line is different in the four experiments; i.e., the relative amounts of the different conformers undergoing excitation in the four experiments are different.

One might think that the remote switching occurs not because of a long-range IVR process but simply due to statistical energy distribution of the absorbed energy, i.e., due to heating. This can, however, easily be excluded by a simple consideration. The computed heat capacity (B3LYP/6-31++G**, anharmonic) of our model compound is 329 J mol^{-1} K^{-1}. This corresponds to a statistical energy distribution (kT) of only ∼220 K, which is only ∼150 cm^{-1}. This means that to trigger a *trans*−*cis* conformation change over a ca. 5000 cm^{-1} *trans* to *cis* barrier[33] the 2νOH absorption should occur at least ∼30 times before the energy is dissipated to the matrix. This is more than a highly unlikely event with our relatively low-power, unfocused laser beam! In addition, the relatively large quartic force constants (4.9 and −4.9 aJ amu^{-2} $Å^{-2}$, for k_{xyyy} and k_{xxxy}, respectively, where x and y denote the two OH stretching normal modes) obtained by VPT2 theory also suggest that the IVR process is feasible between the two groups.

One can also consider that the *trans*−*cis* conformers may be produced not by a remote switching effect but by nonresonant pumping of 2νOH **2**. Such nonresonant pumping, due to coupling of molecular vibrations with phonon modes, was observed for formic acid when it was pumped at the blue side of its OH stretching overtone.[14] The efficiency of this pumping was observed to be 2−3 orders of magnitude weaker than that of the direct pumping. First, in our case, the difference in the efficiency of the local and remote pumping is smaller. Second, the action spectrum (or reactive vibrational excitation, i.e., the integrated band intensities of the high-wavenumber C═O stretching of *trans*−*cis* forms vs excitation frequency; see the Supporting Information) shows that upon irradiation at ∼6980 cm^{-1}, on the red side of the 2νOH **1 II**−**VI** bands, no *trans*−*cis* conformers could be observed. This proves that the *trans*−*cis* forms generated by nonresonant pumping of the 2νOH **2** bands around 2νOH **1 II**−**VI** bands are below our detection limit.

Unfortunately, the long-range IVR process in the other direction (i.e., excitation of group **2** and inducing conformational change in group **1**) cannot be proved on the basis of the carbonyl stretching mode, because, as was mentioned, the carbonyl bands of the *cis*−*trans* forms overlap with those of the *trans*−*trans* conformers.

Although in the other regions of the spectrum the separation of the bands of the *cis*−*trans* and *trans*−*cis* forms are not large enough for unambiguous structural identifications (see computed transitions in the Supporting Information), most of the bands that can be assigned to a short-lived conformer appear at the same position upon the four irradiation experiments but with different relative intensities. This observation suggests that all of the short-lived *cis*−*trans* and *trans*−*cis* forms can be prepared regardless of which carboxylic group (**1** or **2**) is irradiated; i.e., it points to efficient long-range IVR in both directions (excitation of **1** and conformational change in **2**, and *vice versa*).

In order to determine the lifetime of the identified *trans*−*cis* conformers, the time evolution of their most intensive bands was monitored in the dark, after irradiation at 6961 cm^{-1} (see Figure 7). Since no single bands can be unambiguously assigned to the *trans*−*cis* conformers with a given backbone conformation (**I**−**VI**), and also because the signal-to-ratio is low, the absorbances of the bands between 1814 and 1793 cm^{-1} were integrated together. This resulted in an average lifetime of the *trans*−*cis* conformers with different backbone structures of 12 s. This lifetime is comparable with the 7 s lifetime of the glycine **VI** conformer,[21] which can convert via a similar tunneling mechanism to glycine conformer **I**.[33] In a

DOI: 10.1021/acs.jpca.7b00615
J. Phys. Chem. A XXXX, XXX, XXX−XXX

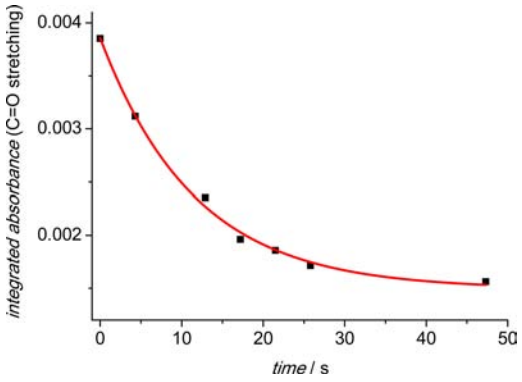

Figure 7. Decay of the CO stretching band of *trans*−*cis* conformers integrated over the bands corresponding to backbones **I**−**VI** and over different sites in Ar matrix.

good correspondence with this, the barriers computed at the MP2/6-311++G** level for the relaxation of the *trans*−*cis* conformer **I** into the *trans*−*trans* conformer **I** in *E*-glutaconic acid and for the relaxation of glycine **VI** conformer into glycine **I** are very similar, amounting to 2045 and 2147 cm^{-1}, respectively.

Former studies have shown that the *cis* conformers of carboxylic acids are stabilized in a N_2 matrix compared to an Ar matrix.[33−37] Due to this stabilization, the lifetime of the *cis* conformers is 2−3 orders of magnitude larger in N_2 matrix. Therefore, it seemed to be an obvious choice to investigate the IVR process in *E*-glutaconic acid in a N_2 matrix. Unfortunately, the OH stretching overtones of the two carboxylic groups are overlapping in this matrix, which made it impossible to excite selectively each one of the two groups.

5. CONCLUSION

In this paper, the long-range IVR process was examined on *E*-glutaconic acid isolated in solid argon. It has been shown that in this model compound a conformational change highly likely occurs in a group separated by eight covalent bonds from the group absorbing the NIR photon. Other long-range IVR driven conformational transformations were formerly identified by the MI method only in more rigid molecules containing aromatic rings.[7−9] Long-range IVR and thermal conductivity processes were also studied in nanotubes and organic polymers, and small peptides by time-resolved two-dimensional infrared (2DIR) spectroscopy.[6,38,39] Although our method provides evidence on the long-range IVR process only by a "static" observation (i.e., observing the resulted conformational change), and in the present case the observation was challenging, our approach is still much simpler than that of the 2DIR experiments. Therefore, the approach applied in the present study can be used to find the best model systems for more complicated 2DIR studies with which the dynamics of these processes can be explored in detail, and which can unambiguously reveal that the observed conformational change is basically IVR driven and not a simple statistical heat effect. Future MI studies on related model compounds can further prove that our observation is not interfered by a larger site-splitting effect.

ASSOCIATED CONTENT

Supporting Information

The Supporting Information is available free of charge on the ACS Publications website at DOI: 10.1021/acs.jpca.7b00615.

The 1500−600 cm^{-1} region of the computed and experimental MIR spectra, action spectrum of the NIR irradiation, Cartesian geometries, computed SQM and VPT2 wavenumbers, and IR intensities of fundamental vibrational transitions of *trans*−*trans*, *cis*−*trans*, and *trans*−*cis* conformers (PDF)

AUTHOR INFORMATION

Corresponding Authors

*E-mail: tarczay@chem.elte.hu.
*E-mail: rfausto@ci.uc.pt.

ORCID

György Tarczay: 0000-0002-2345-1774

Notes

The authors declare no competing financial interest.

ACKNOWLEDGMENTS

This investigation has been performed within the Project PTDC/QEQ-QFI/3284/2014—POCI-01-0145-FEDER-016617, funded by the Portuguese "*Fundação para a Ciência e a Tecnologia*" (FCT) and FEDER/COMPETE 2020-UE. The Coimbra Chemistry Centre (CQC) is supported by FCT, through the project UI0313/QUI/2013, also cofunded by FEDER/COMPETE 2020-UE. N.K. thanks FCT for the postdoctoral grant ref SFRH/BPD/88372/2012 and the Anadolu University (Eskişehir, Turkey), Project 1605F423. The work at Budapest was funded by the Hungarian Scientific Research Fund (OTKA K108649).

REFERENCES

(1) Flynn, G. W.; Parmenter, C. S.; Wodtke, A. M. Vibrational Energy Transfer. *J. Phys. Chem.* **1996**, *100*, 12817−12838.
(2) Boyall, D.; Reid, K. Modern Studies of Intramolecular Vibrational Energy Redistribution. *Chem. Soc. Rev.* **1997**, *26*, 223−232.
(3) Charvat, A.; Aßmann, J.; Abel, B.; Schwarzer, D.; Henning, K.; Luthera, K.; Troe, J. Direct Observation of Intramolecular Vibrational Energy Redistribution of Selectively Excited CH_2I_2 and C_3H_5I Molecules in Solution. *Phys. Chem. Chem. Phys.* **2001**, *3*, 2230−2240.
(4) Kushnarenko, A.; Krylov, V.; Miloglyadov, E.; Quack, M.; Seyfang, G. Intramolecular Vibrational Energy Redistribution Measured by Femtosecond Pump-Probe Experiments in a Hollow Waveguide. *Springer Ser. Chem. Phys.* **2009**, *92*, 349−351.
(5) Schwarzer, D.; Kutne, P.; Schröder, C.; Troe, J. Intramolecular Vibrational Energy Redistribution in Bridged Azulene-Anthracene Compounds: Ballistic Energy Transport through Molecular Chains. *J. Chem. Phys.* **2004**, *121*, 1754−1764.
(6) Rubtsova, N. I.; Qasim, L. N.; Kurnosov, A. A.; Burin, A. L.; Rubtsov, I. V. Ballistic Energy Transport in Oligomers. *Acc. Chem. Res.* **2015**, *48*, 2547−2555.
(7) Halasa, A.; Lapinski, L.; Rostkowska, R.; Nowak, M. Intramolecular Vibrational Energy Redistribution in 2-Thiocytosine: SH Rotamerization Induced by Near-IR Selective Excitation of NH_2 Stretching Overtone. *J. Phys. Chem. A* **2015**, *119*, 9262−9271.
(8) Halasa, A.; Reva, I.; Lapinski, L.; Rostkowska, H.; Fausto, R.; Nowak, M. Conformers of Kojic Acid and Their Near-IR-Induced Conversions: Long-Range Intramolecular Vibrational Energy Transfer. *J. Phys. Chem. A* **2016**, *120*, 2647−2656.
(9) Lopes Jesus, A. J.; Reva, I.; Araujo-Andrade, C.; Fausto, R. Conformational Switching by Vibrational Excitation of a Remote NH Bond. *J. Am. Chem. Soc.* **2015**, *137*, 14240−14243.
(10) Pettersson, M.; Lundell, J.; Khriachtchev, L.; Räsänen, M. IR Spectrum of the Other Rotamer of Formic Acid, *cis*-HCOOH. *J. Am. Chem. Soc.* **1997**, *119*, 11715−11716.

(11) Reva, I. D.; Jarmelo, S.; Lapinski, L.; Fausto, R. IR-Induced Photoisomerization of Glycolic Acid Isolated in Low-Temperature Inert Matrices. *J. Phys. Chem. A* **2004**, *108*, 6982−6989.
(12) Maçôas, E. M. S.; Khriachtchev, L.; Pettersson, M.; Fausto, R.; Räsänen, M. Rotational Isomerization of Small Carboxylic Acids Isolated in Argon Matrices: Tunnelling and Quantum Yields for the Photoinduced Processes. *Phys. Chem. Chem. Phys.* **2005**, *7*, 743−749.
(13) Pettersson, M.; Maçôas, E. M. S.; Khriachtchev, L.; Fausto, R.; Räsänen, M. Conformational Isomerization of Formic Acid by Vibrational Excitation at Energies below the Torsional Barrier. *J. Am. Chem. Soc.* **2003**, *125*, 4058−4059.
(14) Maçôas, E. M. S.; Khriachtchev, L.; Pettersson, M.; Juselius, J.; Fausto, R.; Räsänen, M. Reactive Vibrational Excitation Spectroscopy of Formic Acid in Solid Argon: Quantum Yield for Infrared Induced *trans*→*cis* Isomerization and Solid State Effects on the Vibrational Spectrum. *J. Chem. Phys.* **2003**, *119*, 11765−11772.
(15) Maçôas, E. M. S.; Khriachtchev, L.; Pettersson, M.; Juselius, J.; Fausto, R.; Räsänen, M. Rotational Isomerism of Acetic Acid Isolated in Rare-Gas Matrices: Effect of Medium and Isotopic Substitution on IR-Induced Isomerization Quantum Yield and *cis*→*trans* Tunneling Rate. *J. Chem. Phys.* **2004**, *121*, 1331−1338.
(16) Bazsó, G.; Magyarfalvi, G.; Tarczay, G. Near-Infrared Laser Induced Conformational Change and UV Laser Photolysis of Glycine in Low-Temperature Matrices: Observation of a Short-Lived Conformer. *J. Mol. Struct.* **2012**, *1025*, 33−42.
(17) Najbauer, E. E.; Bazsó, G.; Apóstolo, R.; Fausto, R.; Biczysko, M.; Barone, V.; Tarczay, G. Identification of Serine Conformers by Matrix-Isolation IR Spectroscopy Aided by Near-Infrared Laser-Induced Conformational Change, 2D Correlation Analysis, and Quantum Mechanical Anharmonic Computations. *J. Phys. Chem. B* **2015**, *119*, 10496−10510.
(18) Marushkevich, K.; Khriachtchev, L.; Lundell, J.; Domanskaya, A.; Räsänen, M. Matrix Isolation and Ab Initio Study of Trans−Trans and Trans−Cis Dimers of Formic Acid. *J. Phys. Chem. A* **2010**, *114*, 3495−3502.
(19) Becke, A. D. Density-Functional Thermochemistry. III. The Role of Exact Exchange. *J. Chem. Phys.* **1993**, *98*, 5648−5652.
(20) Lee, C.; Yang, W.; Parr, R. G. Development of the Colle-Salvetti Correlation-Energy Formula into a Functional of the Electron Density. *Phys. Rev. B: Condens. Matter Mater. Phys.* **1988**, *37*, 785−789.
(21) Hehre, W. J.; Ditchfield, R.; Pople, J. A. Self-Consistent Molecular Orbital Methods. XII. Further Extensions of Gaussian-Type Basis Sets for Use in Molecular Orbital Studies of Organic Molecules. *J. Chem. Phys.* **1972**, *56*, 2257−2261.
(22) Francl, M. M.; Petro, W. J.; Hehre, W. J.; Binkley, J. S.; Gordon, M. S.; DeFrees, D. J.; Pople, J. A. Self-Consistent Molecular Orbital Methods. XXIII. A Polarization-Type Basis Set for Second-Row Elements. *J. Chem. Phys.* **1982**, *77*, 3654−3665.
(23) Krishnan, R.; Binkley, J. S.; Seeger, R.; Pople, J. A. Self-Consistent Molecular Orbital Methods. XX. A Basis Set for Correlated Wave Functions. *J. Chem. Phys.* **1980**, *72*, 650−654.
(24) Møller, C.; Plesset, M. S. Note on an Approximation Treatment for Many-Electron Systems. *Phys. Rev.* **1934**, *46*, 618−622.
(25) Peng, C. Y.; Ayala, P. Y.; Schlegel, H. B.; Frisch, M. J. Using Redundant Internal Coordinates to Optimize Equilibrium Geometries and Transition States. *J. Comput. Chem.* **1996**, *17*, 49−56.
(26) Pulay, P.; Fogarasi, G.; Pongor, G.; Boggs, J. E.; Vargha, A. Combination of Theoretical Ab Initio and Experimental Information to Obtain Reliable Harmonic Force Constants. Scaled Quantum Mechanical (QM) Force Fields for Glyoxal, Acrolein, Butadiene, Formaldehyde, and Ethylene. *J. Am. Chem. Soc.* **1983**, *105*, 7037−7047.
(27) Baker, J.; Jarzecki, A. A.; Pulay, P. Direct Scaling of Primitive Valence Force Constants: An Alternative Approach to Scaled Quantum Mechanical Force Fields. *J. Phys. Chem. A* **1998**, *102*, 1412−1424.
(28) Fábri, C.; Szidarovszky, T.; Magyarfalvi, G.; Tarczay, G. Gas-Phase and Ar-Matrix SQM Scaling Factors for Various DFT Functionals with Basis Sets Including Polarization and Diffuse Functions. *J. Phys. Chem. A* **2011**, *115*, 4640−4649.
(29) Frisch, M. J.; Trucks, G. W.; Schlegel, H. B.; Scuseria, G. E.; Robb, M. A.; Cheeseman, J. R.; Scalmani, G.; Barone, V.; Mennucci, B.; Petersson, G. A.; et al. *Gaussian 09*, revision A.1; Gaussian, Inc.: Wallingford, CT, 2009.
(30) *PQS*, version 3.2; Parallel Quantum Solutions: Fayetteville, AR, 2006.
(31) Baker, J.; Wolinski, K.; Malagoli, M.; Kinghorn, D.; Wolinski, P.; Magyarfalvi, G.; Saebo, S.; Janowski, T.; Pulay, P. Quantum Chemistry in Parallel with PQS. *J. Comput. Chem.* **2009**, *30*, 317−335.
(32) Barnes, A. J. Matrix Isolation Vibrational Spectroscopy as a Tool for Studying Conformational Isomerism. *J. Mol. Struct.* **1984**, *113*, 161−174.
(33) Bazsó, G.; Magyarfalvi, G.; Tarczay, G. Tunneling Lifetime of the ttc/VIp Conformer of Glycine in Low-Temperature Matrices. *J. Phys. Chem. A* **2012**, *116*, 10539−10547.
(34) Domanskaya, A. V.; Marushkevich, K.; Räsänen, M.; Khriachtchev, L. Spectroscopic Study of *cis*-to-*trans* Tunneling Reaction of HCOOD in Rare Gas Matrices. *J. Chem. Phys.* **2009**, *130*, 154509.
(35) Lopes, S.; Domanskaya, A. V.; Fausto, R.; Räsänen, M.; Khriachtchev, L. Formic and Acetic Acids in a Nitrogen Matrix: Enhanced Stability of the Higher-Energy Conformer. *J. Chem. Phys.* **2010**, *133*, 144507.
(36) Bazsó, G.; Najbauer, E. E.; Magyarfalvi, G.; Tarczay, G. Near-Infrared Laser Induced Conformational Change of Alanine in Low-Temperature Matrixes and the Tunneling Lifetime of Its Conformer VI. *J. Phys. Chem. A* **2013**, *117*, 1952−1962.
(37) Nunes, C. M.; Lapinski, L.; Fausto, R.; Reva, I. Near-IR Laser Generation of a High-Energy Conformer of L-Alanine and the Mechanism of its Decay in a Low-Temperature Nitrogen Matrix. *J. Chem. Phys.* **2013**, *138*, 125101.
(38) Yu, C.; Shi, L.; Yao, Z.; Li, D.; Majumdar, A. Thermal Conductance and Thermopower of an Individual Single-Wall Carbon Nanotube. *Nano Lett.* **2005**, *5*, 1842−1846.
(39) Hamm, P.; Lim, M. H.; Hochstrasser, R. M. Structure of the Amide I Band of Peptides Measured by Femtosecond Nonlinear-Infrared Spectroscopy. *J. Phys. Chem. B* **1998**, *102*, 6123−6138.

DOI: 10.1021/acs.jpca.7b00615
J. Phys. Chem. A XXXX, XXX, XXX−XXX